Automatic Quantification of the Extracellular Matrix Degradation Produced by Tumor Cells

Nadia Brancati, Giuseppe De Pietro, Maria Frucci, Chiara Amoruso, Daniela Corda and Alessia Varone

Abstract Understanding the mechanisms of invasion of cancer cells into surrounding tissues is of primary importance for limiting tumor progression. The degradation of the extracellular matrix (ECM) and the consequent invasion of the surrounding tissue by tumor cells represent the first stage in the development and dissemination of metastasis. The quantification of such a degradation is thus an important parameter to evaluate the metastatic potential of tumor cells. Assessment of degradation is usually performed in in vitro *assays*, in which tumor cells are cultured on a gelatin (or other matrix)-coated dishes and the degraded gelatin areas under the tumor cells are visualized and quantified by fluorescent labelling. In this paper, we present an automatic method to quantify the ECM degradation through the feature analysis of the digital images, obtained from the in vitro *assays* and showing the tumor cells and the degraded gelatin areas. Differently from the existing methods of image analysis supporting biologists, our method does not require any interaction with the user providing quickly corrected and unbiased measures. Comparative results with a method frequently used by biologists, has been performed.

N. Brancati (✉) · G. De Pietro · M. Frucci
Institute for High Performance Computing and Networking,
National Research Council of Italy (ICAR-CNR), Naples, Italy
e-mail: nadia.brancati@cnr.it

G. De Pietro
e-mail: giuseppe.depietro@cnr.it

M. Frucci
e-mail: maria.frucci@cnr.it

C. Amoruso · D. Corda · A. Varone
Institute of Protein Biochemistry, National Research Council of Italy (IBP-CNR),
Naples, Italy
e-mail: c.amoruso@ibp.cnr.it

D. Corda
e-mail: d.corda@ibp.cnr.it

A. Varone
e-mail: a.varone@ibp.cnr.it

Y.-W. Chen et al. (eds.), *Innovation in Medicine and Healthcare 2016*,
Smart Innovation, Systems and Technologies 60,
DOI 10.1007/978-3-319-39687-3_14

Keywords Extracellular matrix degradation · Binarization · Feature extraction

1 Introduction

The extracellular matrix (ECM) is a highly dynamic structure that is present in all tissues that continuously undergoes controlled remodeling; this is an essential process for development, wound healing and normal organ homeostasis. Many pathological conditions, such as inflammation, cardiovascular disease and tumor cells metastasis, arise when extracellular matrix remodeling becomes excessive or uncontrolled [12]. The analysis and quantification of the ECM degradation by cancer cells is thus a crucial feature to consider in order to determine their metastatic potential [4, 5, 20, 21]. To analyze the invasiveness of tumor cells by means of quantification of the ECM degradation, in vitro *assays* based on cells cultured on a gelatin-coated support, are often used [10]. Measures of the possible degradation of the gelatin matrix allow a quantification of the invasiveness of tumor cells. Different fluorescence substances are generally used to label with different colors the cells and the gelatin support. This process is required to allow the acquisition of two digital images, after a given period of observation of the assay of interest: one image includes only the tumor cells (in the following, cell image), while the second image represents the gelatin support (in the following, gelatin image) located under the tumor cells of the first image (see Fig. 1). The digital images are processed to perform the measure of the degradation areas for each tumor cell. Specifically, segmentation processes of the two acquired images are used to extract the regions of interest (cells and degradation areas, respectively); then, image analysis methods are performed to find both the correspondence between a cell and the relative degradation areas, and the computation of the area of these regions.

Many segmentation methods have been reported for the analysis of biological preparations [3, 8]. They differ in the type of measurements to be carried out [17, 19], in the type of cell images [2, 16] and in the complexity of these images

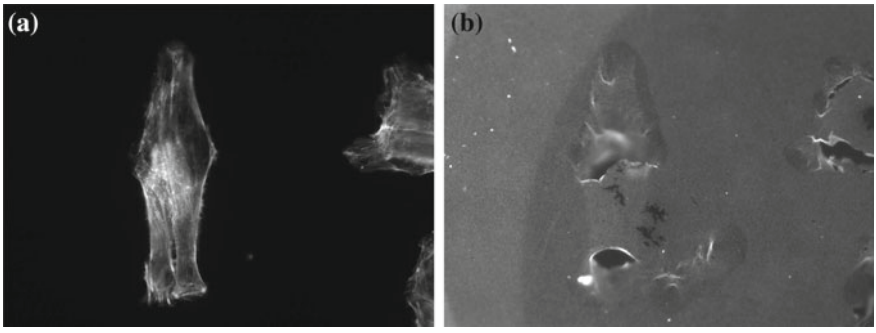

Fig. 1 Example of an assay. **a** Cell image; **b** gelatin image

[18, 22]. In particular, for the types of images of interest in the present study, segmentation processes based on threshold algorithms are commonly adopted: they produce a binary image in which the foreground represents the regions of interest. The binarization processes and the quantification of the degradation areas are performed by means of standardized procedures based on available image processing software [1, 6, 13, 14].

One of the most popular procedures used for this scope, is described in [13] and involves the following steps:

- a manual threshold setting for each binarization process;
- an indication of the feature to compute (for this context, the area);
- the choice of processes to eliminate the noise;
- the selection of the cells for which the degradation areas has to be calculated.

The main limitation of such a procedure is the necessary interaction with the user for the choice of the threshold values to apply in the binarization processes and the methods to remove noise from foreground. Such an interaction can produce arbitrary and subjective measures [7, 9]. In this paper, we propose a method to perform a fully automatic computation of the degradation areas, obtaining quickly results on the whole set of tumor cells under examination.

2 Method

The binarization of the cell image is performed using the faster version [11] of the Multi Otsu Threshold Algorithm [15]. This algorithm requires the definition of the following parameters: the range $[m, M]$ of gray levels in which the threshold values should be computed and the number n of classes in which the image should be partitioned. Generally $m = 0$ and $M = 255$; in this work, the first parameter is automatically defined considering the minimum and maximum values of the gray levels associated to current image. On the basis of the value of the second parameter n, the algorithm provides n threshold values $t_1 = m, t_2 \ldots, t_n < M$. The choice of the second parameter n depends on the type of the image to be segmented. Clearly, a binarization process implies a partition of the image in two classes (foreground and background) and for this, n should be set to 2 to generate a threshold value $m < t_2 < M$; however, the partition performed on the basis of the value t_2 might produce an under or over segmentation. For this, a value $n > 2$ can be appropriate to generate more threshold values and use one of the threshold values or the combination of these values to obtain the correct partition of the image. To obtain the appropriate values of n for both binarization processes, a set of tests has been performed on a dataset of 30 assays, including the digital images of the tumor cells and gelatin supports. Accordingly, the appropriate number n of classes, for the cell images, has been chosen equal to 3. Thus, the algorithm provides three threshold values $t_1 = m$, t_2 and $t_3 < M$; the foreground of the cell image is represented from pixels with gray levels belonging to the range $[t_2, M]$, while the set of remaining pixels represents the background (see

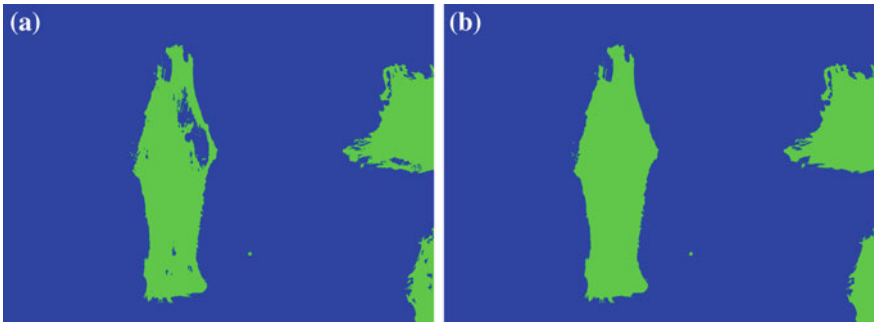

Fig. 2 binarization of the image of Fig. 1. **a** Foreground in *green* and background in *blue*; **b** reduction of noise

Fig. 2a). To reduce the noise in the binarized image, the holes present in the regions of the foreground are filled (see Fig. 2b).

The foreground associated to the cell image is now used as a mask to binarize only the parts of gelatin image in which degradation areas could be detected. In particular, a connected component labeling is performed on the foreground of cell image so that any region of the foreground, representing a cell, is labeled by a single value. For each cell, a new image is built including only the part of the gelatin image corresponding to the selected cell (see Fig. 3a). The same threshold algorithm used for the cell image is applied on this new image, but the values m e M are computed only in the area masked by the current cell and n is experimentally set to 5 to generate five threshold values $t_1 = m, \ldots, t_5 < M$. Since the degradation regions are the dark regions of the images (on the contrary, the cells are lighter than other regions in the relative image), pixels with low gray levels should be taken into account for the detection of the foreground. Precisely, the foreground of the current image is represented from pixels with gray levels belonging to the range $[t_1, (t_2 + t_3)/2]$; the set of remaining pixels represents the background. To eliminate the noise on the found foreground, the same process applied to cell image is carried out (see Fig. 3b). Finally, the area of the foreground is computed.

As soon as the degradation areas of all cells are evaluated, the final result is shown to the user. More precisely, the contours of the cells are outlined in green, and the gelatin degradation areas are visualized in red (see Fig. 4a); moreover, the values of the total degradation area for each cell are given in a table (see Fig. 4b).

Since in some cases, several small degradation areas may not be detected, an optional step to improve the binarization is introduced. In particular, the user can draw a rectangle around the region of interest (ROI). The binarization, with $n = 3$, is performed on the ROI and the foreground is given by the set of pixels with value less or equal to t_2. An example of this improvement process is displayed in Fig. 5.

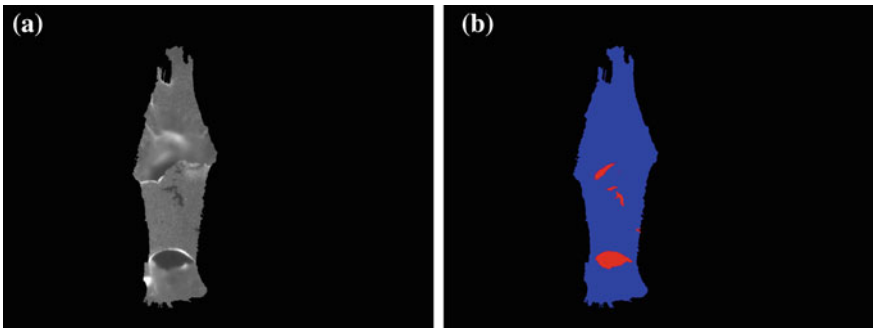

Fig. 3 **a** Gelatin support related to the first cell; **b** binarization with reduction of noise: foreground in *red* and background in *blue*

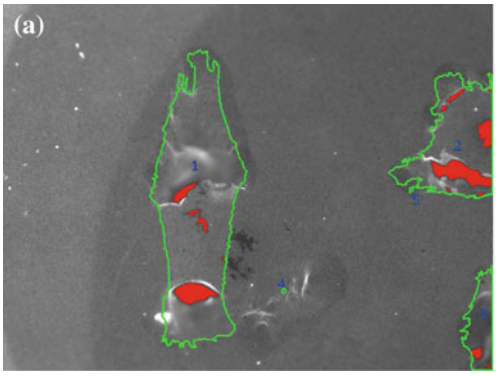

(b)

Region	Area (µm^2)
1	4190.55
2	5772.65
3	4232.57
4	0
5	0

Fig. 4 Result of the detection of the degradation areas. **a** Contours of the cells in *green*, and degradation regions in *red*; **b** measure of the degradation area

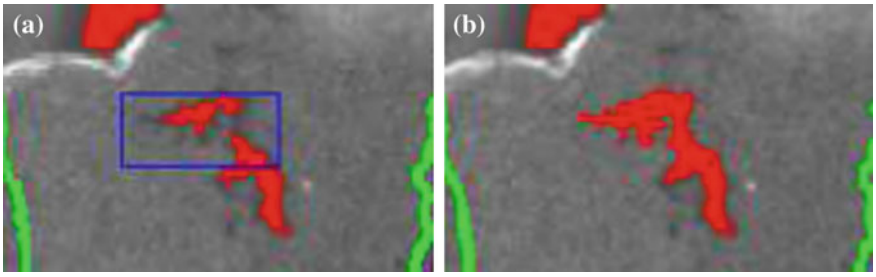

Fig. 5 Example of semi-automatic improvement of the binarization on a magnified part of the Fig. 4a. **a** The *blue rectangle* is defined by the user to obtain a better detection of the degradation area in this part; **b** improved detection of degraded area

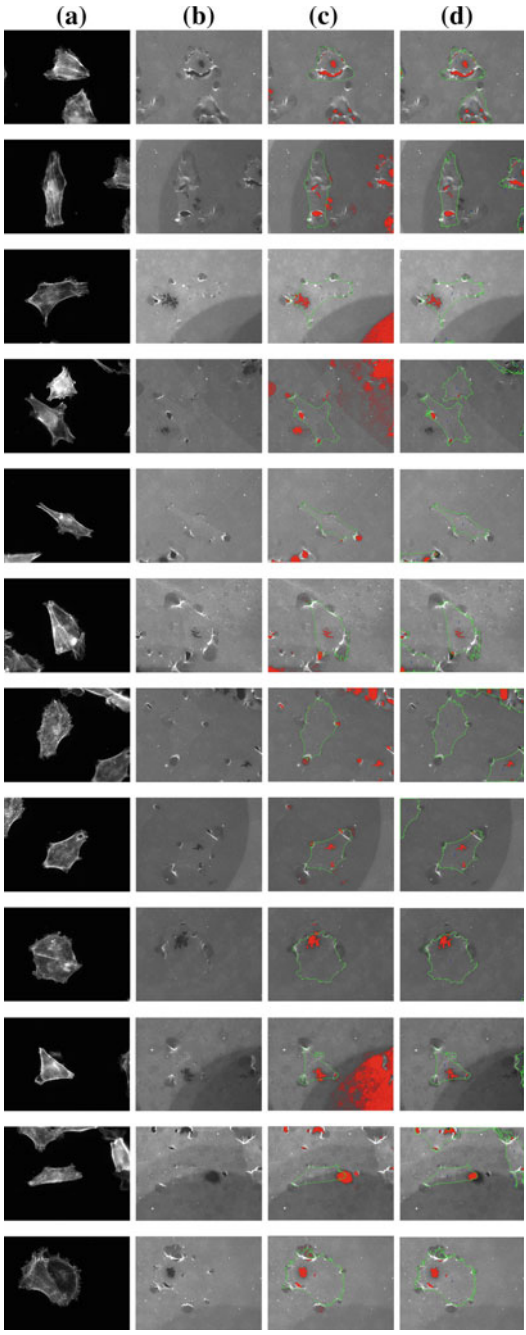

Fig. 6 **a** Cells images; **b** gelatin images; **c** results of the procedure [13] for the cell outlined in *green*. Only the *red* degraded areas included into the selected cell are successively taken into account; **d** results of the proposed, automatic method

3 Results

To evaluate the advantages of the method presented in this study a comparison with the procedure proposed in [13] has been performed. For this, biologists were employed to measure the degradation areas for the dataset of 30 assays, by adopting the standard procedure proposed in [13] and applying, at the same time, our method without taking into account the optional step for the improvement of the binarization. Biologists evaluated the results and confirmed that our method produces generally a comparable or a more accurate detection of degraded areas, for a set of samples large enough. Some examples of the results obtained by applying the two methods are shown in Fig. 6, while comparisons of the quantitative results on the computation of the degradation areas for a given cell, are reported in Table 1. Since different results for the procedure [13] has been obtained by different users, the manual threshold values reported in the Table 1, represent the average of the values provided by biologists employed in the test.

Generally, the threshold values obtained manually for the binarization of the gelatin image are slightly higher than the values automatically computed. This implies that the degradation areas calculated with the procedure in [13] are always a little greater than the ones computed with the method we are reporting. A reason for this phenomenon is partly due to the incorrect human perception of contours of not well defined degraded areas and to the presence of small noisy regions produced by the over segmentation.

According to the overall evaluation of biologists on the use of our method, the advantages can be summarized as follows: (1) the measures can be obtained very

Table 1 Results of the calculation of the degradation areas

	Manual threshold values		Automatic threshold values		Degradation area in μm^2	
Image in row	Cell	Gelatine	Cell	Gelatine	Procedure in [13]	Proposed method
1	15	80	46	77	7677.8	7155.2
2	15	80	42	72	5563.35	4190.55
3	25	90	37	80	6041.75	4442.75
4	30	90	40	69	2654.6	1968.2
5	25	100	45	103	173.55	109.2
6	25	90	41	80	2735.2	1851.2
7	35	80	43	70	289.9	117
8	30	70	44	67	3285.75	2883.4
9	45	60	40	57	7089.55	6268.6
10	45	60	46	65	4767.1	3784.3
11	60	70	46	69	3999.45	3804.45
12	40	90	35	81	6924.45	6002.1

rapidly and consistently; (2) no requirement for selecting a threshold values as for the procedure [13]; (3) reproducibility of the results, independently from the operators; (4) a more accurate identification of the degraded areas.

4 Conclusion

In this paper a fully automatic method for the computation of the ECM degradation areas produced by tumor cells is presented. The method is based on automatic binarization processes of the images obtained on assays of tumor cells cultured on gelatin-coated dishes. Comparisons with the standard semi-automatic procedures reported earlier [13], indicate that the detection and the quantification of the degradation areas are faster and their identification more accurate according to our method; moreover, the choice of parameters is completely unbiased as it is independent from the operators.

References

1. Acerbi, I., Cassereau, L., Dean, I., Shi, Q., Au, A., Park, C., Chen, Y.Y., Liphardt, J., Hwang, E., Weaver, V.M.: Human breast cancer invasion and aggression correlates with ecm stiffening and immune cell infiltration. Integr. Biol. (2015)
2. Arslan, S., Ozyurek, E., Gunduz-Demir, C.: A color and shape based algorithm for segmentation of white blood cells in peripheral blood and bone marrow images. Cytom. Part A **85**(6), 480–490 (2014)
3. Brancati, N., Frucci, M., di Baja, G.S.: Image segmentation via iterative histogram thresholding and morphological features analysis. In: Image Analysis and Recognition, pp. 132–141. Springer (2008)
4. Bravo-Cordero, J.J., Hodgson, L., Condeelis, J.: Directed cell invasion and migration during metastasis. Curr. Opinion Cell Biol. **24**(2), 277–283 (2012)
5. Buccione, R., Caldieri, G., Ayala, I.: Invadopodia: specialized tumor cell structures for the focal degradation of the extracellular matrix. Cancer Metastasis Rev. **28**(1–2), 137–149 (2009)
6. Díaz, B.: Invadopodia detection and gelatin degradation assay. Cancer **3**(24) (2013)
7. Frazer, G.W., Fournier, R.A., Trofymow, J., Hall, R.J.: A comparison of digital and film fisheye photography for analysis of forest canopy structure and gap light transmission. Agric. Forest Meteorol. **109**(4), 249–263 (2001)
8. Frucci, M., Arcelli, C., Di Sanniti, G.: On the hierarchical assignment to the foreground of gray-level image subsets. Int. J. Pattern Recognit. Artif. Intell. **20**(06), 897–912 (2006)
9. Jonckheere, I., Fleck, S., Nackaerts, K., Muys, B., Coppin, P., Weiss, M., Baret, F.: Review of methods for in situ leaf area index determination: part i. Theories, sensors and hemispherical photography. Agric. Forest Meteorol. **121**(1), 19–35 (2004)
10. Kramer, N., Walzl, A., Unger, C., Rosner, M., Krupitza, G., Hengstschläger, M., Dolznig, H.: In vitro cell migration and invasion assays. Mutat. Res./Rev. Mutat. Res. **752**(1), 10–24 (2013)
11. Liao, P.S., Chen, T.S., Chung, P.C.: A fast algorithm for multilevel thresholding. J. Inf. Sci. Eng. **17**(5), 713–727 (2001)
12. Lu, P., Takai, K., Weaver, V.M., Werb, Z.: Extracellular matrix degradation and remodeling in development and disease. Cold Spring Harbor Perspect. Biol. **3**(12), a005058 (2011)

13. Martin, K.H., Hayes, K.E., Walk, E.L., Ammer, A.G., Markwell, S.M., Weed, S.A.: Quantitative measurement of invadopodia-mediated extracellular matrix proteolysis in single and multicellular contexts. J. Vis. Exp. JoVE **66** (2012)
14. Martín-Villar, E., Borda-d'Agua, B., Carrasco-Ramírez, P., Renart, J., Parsons, M., Quintanilla, M., Jones, G.: Podoplanin mediates ecm degradation by squamous carcinoma cells through control of invadopodia stability. Oncogene (2014)
15. Otsu, N.: A threshold selection method from gray-level histograms. Automatica **11**(285–296), 23–27 (1975)
16. Saha, B., Saini, A., Ray, N., Greiner, R., Hugh, J., Tambasco, M.: A robust convergence index filter for breast cancer cell segmentation. In: 2014 IEEE International Conference on Image Processing (ICIP), pp. 922–926. IEEE (2014)
17. Seroussi, I., Veikherman, D., Ofer, N., Yehudai-Resheff, S., Keren, K.: Segmentation and tracking of live cells in phase-contrast images using directional gradient vector flow for snakes. J. Microsc. **247**(2), 137–146 (2012)
18. Su, H., Yin, Z., Huh, S., Kanade, T., Zhu, J.: Interactive cell segmentation based on active and semi-supervised learning (2015)
19. Wang, C.W., Fennell, D., Paul, I., Savage, K., Hamilton, P.: Robust automated tumour segmentation on histological and immunohistochemical tissue images. PloS One **6**(2), e15818 (2011)
20. Weaver, A.M.: Invadopodia: specialized cell structures for cancer invasion. Clin. Exp. Metastasis **23**(2), 97–105 (2006)
21. Yamaguchi, H., Wyckoff, J., Condeelis, J.: Cell migration in tumors. Curr. Ppinion Cell Biol. **17**(5), 559–564 (2005)
22. Yin, Z., Su, H., Ker, E., Li, M., Li, H.: Cell-sensitive microscopy imaging for cell image segmentation. In: Medical Image Computing and Computer-Assisted Intervention–MICCAI 2014, pp. 41–48. Springer (2014)